Synthesis of iron oxyhydroxide-coated rice straw (IOC-RS) and its application in arsenic(V) removal from water

Igor W. K. Ouédraogo, Erol Pehlivan, Hien T. Tran, Yvonne L. Bonzi-Coulibaly, Dieter Zachmann and Müfit Bahadir

ABSTRACT

Because of the recognition that arsenic (As) at low concentrations in drinking water causes severe health effects, the technologies of As removal have become increasingly important. In this study, a simplified and effective method was used to immobilize iron oxyhydroxide onto a pretreated naturally occurring rice straw (RS). The modified RS adsorbent was characterized, using scanning electron microscope, Fourier transform infrared spectroscopy, thermogravimetric analyzer, and surface area analyzer. Experimental batch data of As(V) adsorption were modeled by the isotherms and kinetics models. Although all isotherms, the Langmuir model fitted the equilibrium data better than Freundlich and Dubinin–Radushkevich models and confirmed the surface homogeneity of adsorbent. The iron oxyhydroxide-coated rice straw (IOC-RS) was found to be effective for the removal of As(V) with 98.5% sorption efficiency at a concentration of <50 mg/L of As(V) solution, and thus maximum uptake capacity is ~22 and 20 mg As(V)/g of IOC-RS at pH 4 and 6, respectively. The present study might provide new avenues to achieve the As concentrations required for drinking water recommended by the World Health Organization.

Key words | adsorption, arsenic(V), iron oxyhydroxide, isotherms, rice straw

Igor W. K. Ouédraogo (corresponding author)
Yvonne L. Bonzi-Coulibaly
Laboratoire de Chimie Analytique, Environnementale et Bio-Organique, UFR-SEA,
Université de Ouagadougou,
03 BP 7021 Ouagadougou 03,
Burkina Faso
E-mail: *ouedigor@yahoo.fr*

Erol Pehlivan
Department of Chemical Engineering,
Selcuk University,
Campus,
42031 Konya,
Turkey

Hien T. Tran
Hanoi University of Science,
Hanoi,
Vietnam

Igor W. K. Ouédraogo
Erol Pehlivan
Hien T. Tran
Dieter Zachmann
Müfit Bahadir
Institute of Ecological Chemistry and Waste Analysis, Technical University of Braunschweig,
Hagenring 30,
Braunschweig 38106,
Germany

Igor W. K. Ouédraogo
Biomass Energy and Biofuels Laboratory (LBEB),
International Institute for Water and Environmental Engineering (2iE Foundation),
Ouagadougou 01 01 BP 594,
Burkina Faso

INTRODUCTION

Arsenic (As) is a toxic metalloid which can pollute water, land, crops, and the environment at large, ultimately affecting human health (Zhao *et al.* 2010a, b). A high level of As (>10 mg/L) may cause skin lesions, rhagades, damage mucous membranes, digestive, respiratory, circulatory, nervous system, and moreover it is associated with skin, liver, and lung cancers (Choong *et al.* 2007; Nguyen *et al.* 2009; Lizama *et al.* 2011; Bulut *et al.* 2014). During the last 20 years, naturally occurring As has been found to be widespread in natural water in many countries around the world, especially in Bangladesh, India (West Bengal), China (including Inner Mongolia), Vietnam, Argentina, and some parts of West Africa due to their exposure to high As drinking water sources (Zhang *et al.* 2003; Smedley *et al.* 2007; Pehlivan *et al.* 2013). Works on ground waters from different parts of Burkina Faso have shown that the Yatenga province population has been exposed to As contaminated water with over 0.5–1,600 mg/L (Smedley *et al.* 2007; Barro-Traoré *et al.* 2008).

doi: 10.2166/wh.2015.242

Arsenic cannot be destroyed in the environment; however, it can be changed to different forms and accumulated in different biota and environmental media. Various technologies available for removal of As from contaminated water are based mainly on six principles: (i) oxidation and filtration; (ii) biological oxidation: oxidation of As(III) to As(V) by micro-organisms and then removal of As(V) by iron and manganese oxides; (iii) co-precipitation: oxidation of As(III) to As(V) by adding suitable oxidizing agent followed by coagulation, sedimentation, and filtration; (iv) adsorption: activated alumina, activated carbon, iron-based sorbents, zero-valent iron, and hydrated iron oxide, etc.; (v) ion-exchange through suitable cation and anion exchange resins; and (vi) membrane technology: reverse osmosis, nanofiltration, and electrodialysis (Mondal *et al.* 2006; Lizama *et al.* 2011; Jain & Singh 2012). Among these, a few treatment technologies are efficient but expensive whereas some are cheaper but not efficient. Because of the simplicity of the adsorption process, it has become one of the most promising and applied methods in As removal (Kanel *et al.* 2006; Bulut *et al.* 2014). The most commonly employed adsorbents used for removal of As include magnetic iron oxide nanoparticles (Song *et al.* 2013), activated alumina (Singh & Pant 2004), resin-MnO_2 (Lenoble *et al.* 2004), TiO_2 (Dutta *et al.* 2004), nanostructured ZrO_2 spheres (Cui *et al.* 2013), ores (Chakravarty *et al.* 2002; Zhang *et al.* 2004), zeolites (Elizalde-Gonzalez *et al.* 2001), activated carbon (Kalderis *et al.* 2008), functionalized graphene (Mishra & Ramaprabhu 2011), p(4-vinylpyridine)-based hydrogels (Sahiner *et al.* 2011), iron-modified: resin (Rau *et al.* 2003), sponge (Munoz *et al.* 2002), and sand (Thirunavukkarasu *et al.* 2003). Unfortunately, most of these materials are considered as expensive adsorbent in many countries.

During recent years, interest has been primarily focused on the production of low-cost sorbents from agricultural wastes or byproducts. Lignocellulosic materials are evaluated to be very economic precursors for the production of adsorbents that have been used extensively for many purposes of separation and purification. However, the adsorption capacities of lignocellulose for removing As are low and slow (Amin *et al.* 2006; Elizalde-Gonzalez *et al.* 2008; Urík *et al.* 2009; Ranjan *et al.* 2009; Anirudhan *et al.* 2012). Therefore, chemical modifications have been employed to synthesize appropriated and efficient adsorbents for removing As ions; these include iron-impregnated: biomass (Aryal *et al.* 2010), chitosan (Gupta *et al.* 2009; Gang *et al.* 2010), bead cellulose (BCF) (Guo & Chen 2005), lignocellulose substrate (iron(III)-LS) (Dupont *et al.* 2007), sawdust (Urík *et al.* 2009), and rice husk (RH-FeOOH) (Pehlivan *et al.* 2013).

Rice straw (RS) is one of the most abundant natural sources in the world. Its annual production is about 731 million tonnes, which is distributed in Asia (667.6 million tonnes), America (37.2 million tonnes), Africa (20.9 million tonnes), Europe (3.9 million tonnes), and Oceania (1.7 million tonnes) (Kim & Dale 2004; Binod *et al.* 2010; Hsu *et al.* 2010). It is a kind of lignocellulosic biomass which contains about 32–47% cellulose, 19–27% hemicellulose, and 5–24% lignin (Karimi *et al.* 2006; Wattanasiriwech *et al.* 2010). This material is one of the most agriculture wastes listed in Burkina Faso. In this context, we decided to probe the adsorption capabilities of RS-based matrixes toward As(V).

This paper presents the synthesis of an inorganic–organic hybrid adsorbent of iron oxyhydroxide-coated rice straw (IOC-RS) by RS: (i) pretreatment in sulfuric acid and sodium hydroxide solutions; and (ii) impregnation in ferric nitrate and sodium hydroxide solutions. This work focused on investigating how various experimental parameters influence As(V) adsorption. These parameters included: pH, As(V) initial concentration and the interference of dissolved $NaNO_3$, $MgSO_4$, and Na_3PO_4.

EXPERIMENTAL

Chemicals

H_2SO_4 and NaOH used for RS pretreatment were purchased from Merck. $Fe(NO_3)_3$ procured from Merck was used for biosorbent modification. A Titrisol ampule with As_2O_5 in H_2O used for batch sorption experiments was purchased from Merck, Germany. As(V) stock solution of 1,000 mg/L As(V) was prepared by transferring the Titrisol ampule content with As_2O_5 in H_2O (Merck, Darmstadt, Germany) into a 1 L volumetric flask, which was filled up to the mark at 20 °C and stored at 16 °C. Diluted solutions of As(V) were prepared daily before starting the batch

studies. NH_4OH and HCl purchased from Merck, Germany, were used to adjust the pH solutions. $MgSO_4{\cdot}7H_2O$ (Fluka, Seelze, Germany), $Na_3PO_4{\cdot}12H_2O$ (Sigma-Aldrich, Seelze, Germany) and $NaNO_3$ (Merck) were used for studying the effects of ionic strength. KI used for reduction of As(V) to As(III), was obtained from Roth, Germany. $NaBH_4$ (Fluka, Seelze, Germany), NaOH (Merck, Darmstadt, Germany), and HCl (Merck, Darmstadt, Germany) were used for hydride generation (HG). All reagents used throughout this work were of analytical grade. All glassware was cleaned with diluted nitric acid solution and rinsed with deionized water. Pure water was obtained with a water system filtration (Seralpur, Pro90C).

Pretreatment of raw RS

RS was collected from local farm near the Ouagadougou area, Burkina Faso. The straws were cut into small pieces with lengths of $\leq$6 cm and then washed three times with tap water. The air-dried material (at 60 °C) was made into powder in an electrical ball mill (BLB Braunschweig) and sieved in an electrical sieving machine (Retsh, West of Germany). The particles of sizes between 0.125 and 0.200 mm were rewashed thoroughly with deionized water to remove the fine particles, and dried in a hot-air oven (at 70 °C) for 24 h. The air-dried and powdered RS (60 g) was successively treated with: (i) 2 mol/L H_2SO_4 (1/1 w/w of dry matter, at 80 °C for 30 min) to remove starch, proteins, and sugars; and (ii) 0.5 mol/L NaOH (ratio straw/sodium hydroxide = 5, stirring for 24 h at 22 °C) to remove the low molecular weight lignin compounds after filtration. The substrate was thoroughly washed, and then the material was air-dried in an oven at 60 °C for 24 h. The dried material was stored in a vacuum desiccator.

Preparation of the sorbent

Twenty-five grams of the dry acid and alkali-treated RS was soaking with 100 mL deionized water for 2 h. The soaked substrate was crushed in a porcelain mortar to get a solid paste. Coating was performed by reacting the solid pasty material with 800 mL of ferric nitrate $Fe(NO_3)_3$ solution (0.05 mol/L) in a 2 L flask. Sodium hydroxide (1 mol/L) was slowly added into the mixture, under continuous stirring, until the pH rose to a value between 2.8 and 3.2. The loading process was left for 24 h, and the pH was checked and readjusted with acid (0.1 mol/L HCl) and base (0.1 mol/L NaOH) solutions during the process. The sorbent was then filtered, washed with deionized water several times, dried in an oven at 50 °C for 24 h and stored in desiccators.

Methods of characterization

The thermogravimetric analysis (TGA) of RS and IOC-RS were analyzed using a SETSYS Evolution TGA 16/18 Setaram Instrumentation. The ramping rate was 10 °C/min up to 900 °C in a nitrogen environment. The scanning electron microscope (SEM) was performed on JEOL JSM-6480 microscope to collect the SEM images of the adsorbents. The Fourier transform infrared spectroscopy (FTIR) was carried out on a Bruker Tensor 27 spectrometer, Diamant attenuated total reflectance. The spectra were recorded in the region of 4,000–520 cm^{-1} for 32 scans. The specific surface area was determined by N_2 adsorption at −196 °C using an ASAP 2020 Micromeritics instrument and the Brunauer–Emmett–Teller method (Sing *et al.* 1985). The zeta potential measurement of the sorbent was performed by mixing 0.2 g of sample with 50 mL of deionized water at 22 ± 2 °C. The pH_i (initial pH) values of the solution were adjusted roughly from pH 4 to 10 by a pH meter, via addition of 0.1 M HCl or NH_4OH. The mixture was shacked to the equilibrium time of 4 h. After completion of the equilibration time, the admixture was filtered and the pH_f (final pH) values were measured. The difference between pH_i and pH_f values ($\Delta pH = pH_f - pH_i$) was plotted versus the pH_i. The pH value at the point of zero charge (pH_{pzc}) of the sorbent was determined from the point of intersection of the resulting curve, at which $\Delta pH = 0$. For As(V) concentrations access, HG attached with atomic absorption spectrometry with a Zeeman correction (AAS-Hitachi Z-2000) was used, with a calibration range from 1 to 20 μg/L. Arsine obtained from As(III) gives the best signal; therefore, all As(V) in the sample was previously reduced to As(III). The reduction was carried out with the optimized protocol: 30% HCl (2.5 mL) and 20% KI (2.5 mL) solution as a reduction agent were added to all sample solutions (10 mL), and a waiting time of 1 h allowed for complete reduction of As(V); then the whole were made up to 25 mL before

analysis. For HG, the following solutions were used: (i) 1.2 M HCl; and (ii) $NaBH_4$–NaOH solution (solute 10 g $NaBH_4$ in 1 L of H_2O Seralpure by adding 4 g of NaOH); the solution was prepared immediately before use. The principle is to volatilize As from As(III) to arsine AsH_3(g), due to a reaction of nascent hydrogen on As. This nascent hydrogen comes from the decomposition of BH_4^- ions.

Batch sorption experiments

Batch experiments were performed in plastic bottles (50 mL) by adding the sorbent in 50 mL of aqueous As(V) solution of the desired initial pH. For all experiments, the initial pH of the As(V) solution was controlled every 30 min with a digital pH meter by adding 0.1 M HCl and/or NH_4OH solution as required. The bottles were gently agitated with a rotary shaker (Retsch, Berlin, Germany) at 120 rpm. The sorbent was separated by filtration with cellulosic acetate film (pore size 0.2 μm) and the remaining As was analyzed using HG atomic absorption spectrometry. Each experiment was replicated three times at the desired initial conditions and the mean (average) values are taken. The amount of As(V) adsorption at equilibrium, q_e (mg/g), was calculated using the following equation:

$$q_e = (C_0 - C_e)\frac{V}{W} \quad (1)$$

where C_0 and C_e are the As concentrations (mg/L) initially and at equilibrium, respectively. V is the volume of the As(V) solutions (L), and W is the weight of sorbent (g). q_e (mg/g) is the adsorption capacity at equilibrium.

Effect of solution initial pH on As(V) sorption

The effect of solution pH was carried out by adding 0.2 g of sorbent in 50 mL of As(V) solution of 50 mg/L initial concentration at different pH values (2.0–10.0). The mixture was gently agitated with a rotary shaker (Retsch, Berlin, Germany) for 8 h at a temperature of 22 ± 2 °C.

Effect of initial concentration and ionic strength on As(V) sorption

The influence of initial solution concentration on As(V) sorption with sorbent was carried out by adding 0.2 g of sorbent into 50 mL of As(V) solution of 10–300 mg/L initial concentration. The pH values were adjusted at 4 and 6, and the mixtures were shaken for 24 h at 22 ± 2 °C. The As sorption experiments were repeated with solution containing the mixture ions of dissolved $NaNO_3$, $MgSO_4$, and Na_3PO_4, usually present in water with As(V) solution of 50 mg/L.

RESULTS AND DISCUSSION

Sorbent characterization

The SEM pictures (Figure 1) reveal the surface textures and porosities of RS and IOC-RS. It was found that after the surface of RS had been coated by the iron oxyhydroxide in the iron reclaim system, the apparent color of RS changed from dark yellow to dark orange (red), and the surface morphology became much finer and smoother. On the other hand,

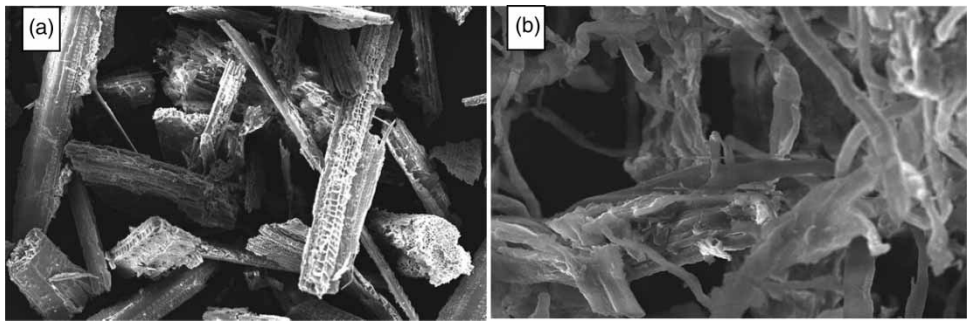

Figure 1 | SEM of (a) RS and (b) IOC-RS.

the surface area of the IOC-RS (7.86 m^2/g) was also different from that of RS (2.85 m^2/g).

RS is a lignocellulosic (cellulose, hemicellulose, and lignin) and silica matrix, which likely consists of alkene, esters, aromatic, ketones, and alcohols with different oxygen-containing functional groups. The FTIR spectrum of RS (Figure 2(a)) showed bands at 897 cm^{-1}, 1,060 cm^{-1}, and 1,380 cm^{-1}, which are ascribed to β-glycosidic linkages, C–O–C stretching and O–H bending, respectively (Sun *et al.* 2004). The bands observed at 3,332 cm^{-1} and 1,735 cm^{-1} can be assigned to O–H stretching and C=O stretching, respectively. The presence of C=C groups is reflected by vibration bands at 1,606 and 1,515 cm^{-1} due to aromatic rings of lignins (Fernandez-Bolanos *et al.* 1999). On the other hand, the adsorption peaks at 1,645 cm^{-1} and 796 cm^{-1} are, respectively, assigned to the H–O–H bending mode (Liu *et al.* 2006) and the symmetric Si–O–Si stretching vibration (Farook *et al.* 2006). The loaded RS spectrum (Figure 2(b)) shows some changes mainly in the decrease of the peak intensities at 1,735 and 1,645 cm^{-1}, which can be explained by the complexation of Fe^{3+} ions with carboxylate and hydroxyl groups in the matrix (Pehlivan *et al.* 2013). The decrease of peaks observed at 1,606, 1,515, and 796 cm^{-1} is due to a partial removal of lignins and silica during the pretreatment with NaOH (Sun *et al.* 2004; Liu *et al.* 2006). The strong band between 600 and 520 cm^{-1} belongs to the stretching mode Fe–O (Correa *et al.* 2010; Bordoloi *et al.* 2013; Bulut *et al.* 2014).

The thermal degradation (Figure 3) of RS and IOC-RS showed that there was a similar weight loss between 150 and 550 °C due to degradation of lignocellulose polymers. The minor weight loss of ~1.5% was first observed around 160 °C in the RS, which may be due to the decomposition of volatile matters such as low molecular weight sugars. Following this, a substantial weight loss by ~50% took place from 200 to 400 °C. This was expected to be the decomposition of hemicellulose and cellulose (Wattanasiriwech *et al.* 2010); the overlapping peaks in the differential thermogram (DTG) are, respectively, 322 and 366 °C. Another important loss of ~14% due to the decomposition of lignin occurred between 350 and 540 °C. For IOC-RS, the result clearly shows that the thermal stability changed by modification of RS with iron. The DTG shows one peak at 354 °C, suggesting that it was likely that hemicellulose and cellulose simultaneously decompose within this temperature. The percentage weight loss of the residue after heating up to 700 °C was ~4% higher for IOC-RS when compared to unmodified RS. This implies that there was presence of iron in IOC-RS

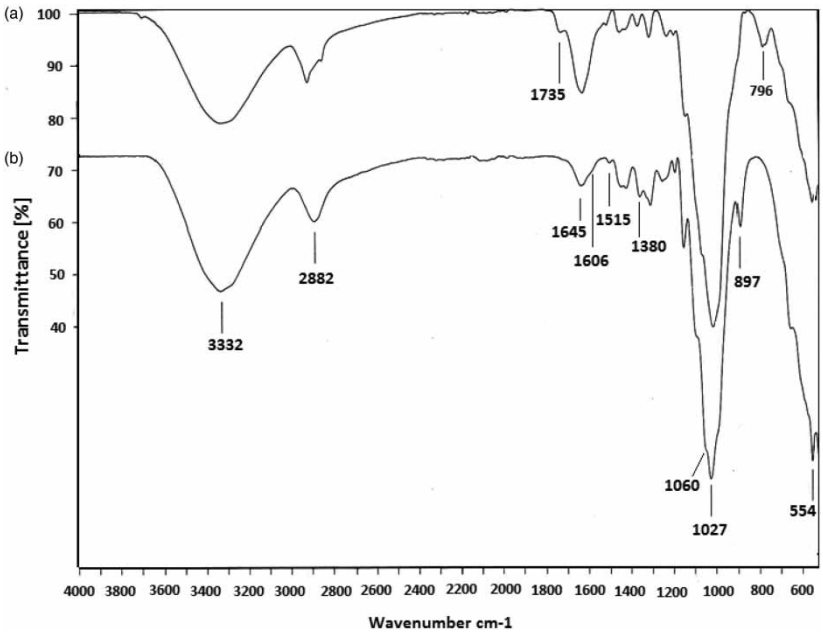

Figure 2 | FTIR spectra of (a) RS and (b) IOC-RS.

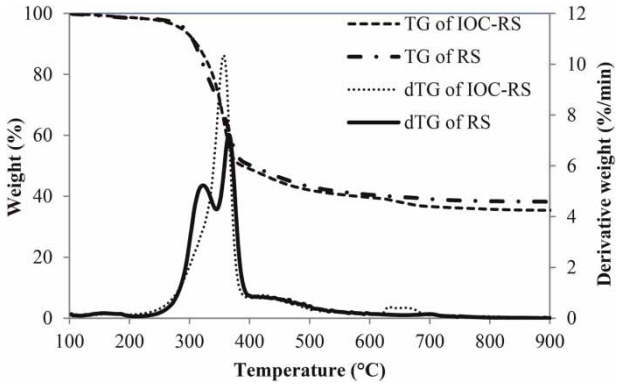

Figure 3 | TGA and DTG thermograms of RS and IOC-RS.

which was not degraded when the samples were heated up to 700 °C. In addition, it was found that ash content in the pretreated RS was only 3.53% whereas that in the IOC-RS was increased to 22.84%; this higher percentage of residual ash in IOC-RS is assumed to be from iron(III)–lignocellulose complex. The form of iron in the IOC-RS was iron oxyhydroxide (–FeOOH), as previously reported (Pehlivan *et al.* 2013).

The pH_{zpc} (zero proton charge (zpc)) of an adsorbent is a very important characteristic that determines the pH at which the sorbent surface has net electrical neutrality, and at which value the acidic or basic functional groups no longer contribute to the pH of the solution (Wan Ngah & Hanafiah 2008). Figure 4 shows a plot of the zeta potential (ΔpH) of sorbent versus initial pH (pHi). The values of the zeta potential in all suspensions decreased as the pH was increased. According to the zeta potential curve of sorbent, it was found that the pH_{zpc} of IOC-RS was about 5.9. This result is in agreement with the pH_{zpc} of Fe(III)-coated rice husk (Pehlivan *et al.* 2013). Based on the pH_{zpc} value, it can be deduced that the IOC-RS surface charge is globally positive, as the solution pH is less than 6. On the contrary, with a solution pH higher than the pH_{zpc}, the surface is negatively charged and there will be an electrostatic repulsion between an anionic species and the surface of IOC-RS.

The effect of solution initial pH on As(V) sorption

To determine the optimum pH for adsorption of As over RS and IOC-RS, the uptake of As(V) was studied at pH range of 2–10 and the removal data are shown in Figure 5. Results from the present study clearly show that As(V) adsorption by RS is not effective whatever the solution pH; while the percent removal of As(V) by IOC-RS was reduced from 99.6 to 64.3% as pH shifted from 2 to 10. Optimal As(V) adsorption by IOC-RS was found in the range of pH 2–4 in which the removal rate was above 95%. The pH affects significantly the speciation of As(V) in solution and the surface charge of the solid particles. As(V) species and their corresponding stability pH values are H_3AsO_4 (pH <2), $H_2AsO_4^-$ (pH 2–7), $HAsO_4^{2-}$ (pH 7–11), and AsO_4^{3-} (pH >12). As pH increased from 4 to 10, the amount of multivalent species ($HAsO_4^{2-}$ (pH 5–9) and AsO_4^{3-} (pH >9)) increased and the two species were not preferably adsorbed by IOC-RS in comparison with $H_2AsO_4^-$.

It was previously reported that the main factors governing the adsorption of As species are (i) the electrostatic interaction between iron oxyhydroxide sites of the adsorbent surface and (ii) the anionic As(V) species (Pehlivan

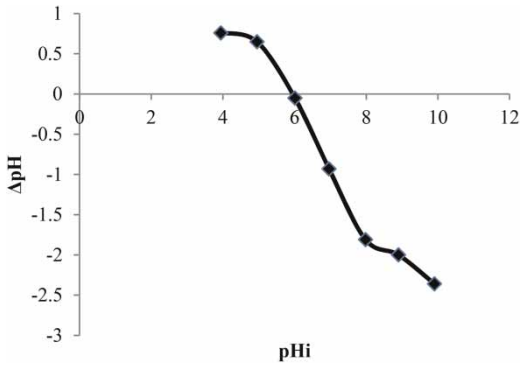

Figure 4 | Plot of ΔpH against pH_i of IOC-RS. Experimental conditions: sorbent amount = 4 g/L, ultrapure water pH range = 4–10, shaking time = 4 h, temperature = 22 ± 2 °C.

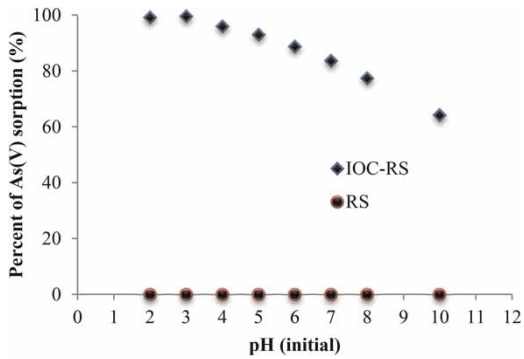

Figure 5 | Effect of pH on the adsorption of As(V) with RS and IOC-RS. Experimental conditions: initial arsenate concentration = 50 mg/L, sorbent amount = 4 g/L, pH range = 2–10, temperature = 22 ± 2 °C, shaking time = 8 h.

et al. 2013). As the equilibrium pH increased from lower pH to pH_{zpc}, the decreased percentage removal of As(V) was attributed to the decreasing electrostatic attraction between the surface of iron oxyhydroxide loaded in IOC-RS and anionic multivalent $HAsO_4^{2-}$ and AsO_4^{3-} species. Over the pH_{zpc} value, the surface sites of IOC-RS were negatively charged and inappropriate for adsorbing anionic arsenate species. The decrease in arsenate adsorption at pH > pH_{zpc} may have been due to the increase in the negative charge density at the surface of the adsorbent, and to the increase in the number of OH^- ions in the solution, in competition with the anionic arsenate species for adsorption.

The effect of initial concentration and isotherm study

To be able to estimate maximum capacities of adsorbents, it is necessary to know the quantity of adsorbed As(V) as a function of As(V) concentration in solution. The As(V) adsorption isotherms for the sorbent are shown in Figure 6. The sorption data obtained were analyzed by fitting the Freundlich and Langmuir isotherm models (Ranjan et al. 2009; Mishra & Ramaprabhu 2011; Maji et al. 2013). Table 1 gives a full overview of the Freundlich and Langmuir adsorption isotherm parameters.

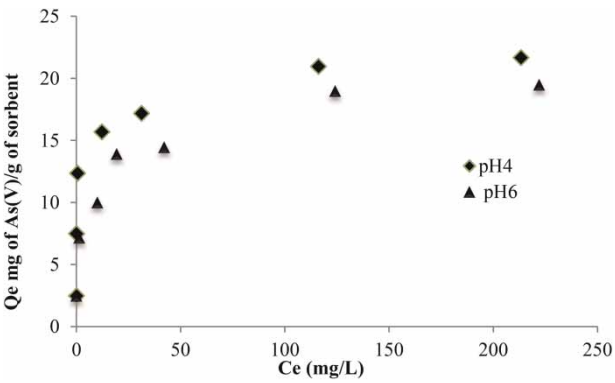

Figure 6 | Effect of initial As(V) ion concentration on the adsorption of As(V) ion with IOC-RS. Experimental conditions: initial arsenate concentration range (10–300 mg/L), pH = 6 and 4, sorbent amount = 4 g/L, adsorption temperature = 22 ± 2 °C, shaking time = 24 h.

The Freundlich isotherm is most frequently used to describe the adsorption of heavy metal ions in solution. The Freundlich isotherm assumes that the uptakes of metal ions occur on a heterogeneous surface by multilayer adsorption. The equilibrium data were analyzed using the following Freundlich equation:

$$\ln q_e = \ln K_f + \left(\frac{1}{n}\right) \ln C_e \tag{2}$$

where $1/n$ is the intensity of adsorption, K_f is the adsorption capacity, q_e is the amount of As(V) adsorbed per unit amount of the adsorbent (mg/L), and C_e is the equilibrium concentration in solution. The K_f and $1/n$ values are calculated from the linear plot of ln q_e versus ln C_e (Table 1). The $1/n$ value was between 0 and 1 indicating that the sorption of As(V) using understudy sorbent material was favorable at the studied conditions. However, the R^2 value was found to be >0.9784, indicating that the Freundlich model was applicable for the relationship between the amounts of As(V) ions sorbed and its equilibrium concentration in the solution.

The Langmuir model has eventually been empirically the best known of all sorption isotherms used since it contains the two useful and easily imaginable parameters (b and Q) which are more easily understandable. A basic assumption of this theory is that sorption takes place at specific homogeneous sites within the sorbent. This model can be written in linear form

$$\frac{C_e}{q_e} = \frac{C_e}{Q} + \frac{1}{Qb} \tag{3}$$

Table 1 | Freundlich, Langmuir, and Dubinin–Radushkevich (D–R) characteristic constants for As(V) adsorption onto IOC-RS

	Freundlich isotherm model			Langmuir isotherm model			D–R isotherm model			
pH	K_f (mg/g)(L/mg)^n	$1/n$	R^2	Q (mg/g)	R^2	R_L	Xm (mol/g)	β (mol^2/kJ^2)	R^2	E (kJ/mol)
4	12.7457	0.0971	0.9784	21.739	0.9985	0.026	0.00035	−0.001	0.9791	22.36
6	6.8264	0.2039	0.9687	19.960	0.9961	0.064	0.00029	−0.0008	0.9778	25.00

where C_e is the equilibrium concentration of As(V) (mg/L) in solution, q_e is the amount of As(V) (mg/g) adsorbed per unit mass of adsorbent, and Q is the monolayer sorption saturation capacity (mg/g). b (L/mg) is a constant related to the affinity of binding sites or bonding energy.

A plot of C_e/q_e versus Ce is given in a straight line with its slope of $1/Q$ and intercept of $1/Qb$ and the results are shown in Table 1. According to the coefficients of correlation obtained ($R^2 > 0.9961$), the sorption of As(V) ions onto sorbent material, are fitted well to the Langmuir model. The maximum adsorption capacity of sorbent material for As(V) removal at pH 6 and 4 were found to be 19.96 mg/g and 21.739 mg/g, respectively (Table 1). Recently, several studies related to As(V) ions adsorption from water used for drinking and irrigation of crops have been carried out. Table 2 compares As(V) adsorption capacities of iron-based material adsorbents reported in previous studies. As seen, iron(III)-loaded resin has a high adsorption capacity for As(V) at pH < 2. In comparison to these approaches, the IOC-RS material (at pH 6) reported herein achieved better results than the amorphous iron oxide and ferric oxyhydroxides-modified sawdust, displaying at least five-fold better removal efficiency than the iron oxide nanoparticles and iron(III)-coated rice husk and a higher efficiency compared to the iron ores, iron oxide-coated sand (IOCS) and zeolite (ICZ). On the other hand, it was also found that the adsorption capacities of IOC-RS carried out at pH 4 and 6 are, respectively, comparable to those of iron-coated chitosan flakes (ICF) (pH 7) and iron(III)-loaded sponge (pH 9). The content of iron in the matrix is a crucial factor which impacts on the As adsorption capacity. In our case, there was a significant increase of ash content, which indicates high amounts of iron adsorbed on the surface of the RS substrate compared to the reported rice husk. This could relate to the chemical and physical properties of the feedstock. Rice husk is made of hard materials, including opaline silica and lignin, and has a more recalcitrant cell wall structure than RS, which contains a lesser amount of lignin (Boonmee 2012). In a future study, the correlation between the amount of iron-coated RS and the As adsorption capacity will be investigated. Moreover, it was found that IOC-RS could be regenerated by HCl and NaOH treatment. The highest recovery of >88% was achieved with 1 M NaOH.

To determine that the nature of sorption processes is physical or chemical, the equilibrium data were also modeled using the Dubinin–Radushkevich (D–R) isotherm

Table 2 | Removal capacities of the iron-based sorbents towards As(V)

Matrix	Removal capacity (mg of As(V)/g)	pH controlled	References
IOC-RS	21.74	4	This study
	19.96	6	This study
Amorphous iron oxide	7.12		Lenoble *et al.* (2002)
Fe(III)-coated rice husk	2.47	4	Pehlivan *et al.* (2013)
Ferric oxyhydroxide-modified sawdust	9.29	8	Urík *et al.* (2009)
Magnetic iron oxide nanoparticles	3.07	6	Song *et al.* (2013)
Iron ores	0.37	4.5–6.5	Zhang *et al.* (2004)
IOCS	0.41	7.6	Thirunavukkarasu *et al.* (2003)
ICZ	0.67	4	Jeon *et al.* (2009)
Iron-coated chitosan beads	0.25	7	Gupta *et al.* (2009)
Fe(III)-loaded sponge	17.98	9	Munoz *et al.* (2002)
ICF	22.48	7	Gupta *et al.* (2009)
BCF impregnated with Fe oxide hydroxide (BCF)	33.19	7	Guo & Chen (2005)
Fe(III)-loaded resin	59.94	1.7	Rau *et al.* (2003)

equation (Namasivayam & Sureshkumar 2008; Baig *et al.* 2010) as follows:

$$\ln q_e = \ln Xm - \beta\varepsilon^2 \tag{4}$$

where

$$\varepsilon = RT\ln\left(1+\frac{1}{C_e}\right) \tag{5}$$

where q_e is the amount of As ions adsorbed on per unit weight of sorbent material (mol/g), and Ce is the concentrations at equilibrium (mol/L). Xm is the maximum sorption capacity (mol/g), β is the activity coefficient (mol^2/kJ^2) related to sorption mean free energy (kJ/mol), and ε is the Polanyi potential, where R (8.32 J/mol/K) is the gas constant and T (K) is the absolute temperature. The constant β and Xm (Table 1) were estimated from slope and intercept of the plot of ln q_e against ε^2. The R^2 value shows that the present data describe well the D–R equation.

The mean free energy of adsorption (E), defined as free energy change when 1 mol of As(V) ion is transferred from infinity in solution to the surface of IOC-RS, can be calculated using the value of β, according to the following equation:

$$E = (-2\beta)^{-1/2} \tag{6}$$

It was reported that when the magnitude of E is: (i) less than 8 kJ/mol, physical adsorption is the major process; (ii) between 8 and 16 kJ/mol, the adsorption behavior is dominated by ion-exchange; and (iii) in the range of 20–40 kJ/mol, chemisorption is predominant in the adsorption procedure (Han *et al.* 2013). The estimated values of E (Table 1) obtained at pH 4 and 6 were respectively 22.36 and 25 kJ/mol, suggesting that the sorption of As(V) ion on the surface of IOC-RS took place with chemisorption mechanism.

Effect of concomitant ions

The sorption of As(V) in the presence of common anions ions may be affected due to precipitation, complex formation or competition for sorption sites. Interference of anions on the sorption of As(V) onto sorbent was carried out with As(V) solution containing 50 mg/L of anion (i.e., NO_3^-, SO_4^{2-}, or PO_4^{3-}) ions, at pH 4. It was observed that except for PO_4^{3-}, other ions, e.g., NO_3^- and SO_4^{2-} have no significant interference with sorption of As(V) ions. The decrease of percentage removal of As(V) in the presence of PO_4^{3-} was 6%.

CONCLUSION

In this work, an inorganic–organic hybrid IOC-RS was used as adsorbent for the removal of As(V) from aqueous solution. The major conclusions based on the experimental study were as follows:

1. The pH, contact time, initial concentration, and dissolved Na_3PO_4 on the adsorption, significantly affect the As(V) adsorption capacity of IOC-RS.
2. The isotherm modeling revealed that the Langmuir equation could better describe the adsorption of As(V) on the IOC-RS as compared to Freundlich and D–R models. The maximum adsorption capability of IOC-RS reached ~22 mg As(V)/g of IOC-RS at pH 4.0 and 22 °C. In addition, the adsorption energy indicates that the adsorption process is dominated by the chemisorption.
3. The removal capacity Q of IOC-RS sorbent for As(V) ions was found to be higher than that of the majority of other iron oxide sorbents reported in the literature. Therefore, it can be stated that this sorbent has significant potential for the removal of As(V) ions from natural water.

ACKNOWLEDGEMENTS

This investigation was performed at the Guest Chair within the project 'Exceed – Excellence Center for Development Cooperation – Sustainable Water Management in Developing Countries' at the Technische Universitaet Braunschweig, Prof. Pehlivan being the visiting professor, and Ms Tran and Dr Ouédraogo being the international exchange staff members. The Exceed Project is granted by the German Federal Ministry for Economic Cooperation and Development (BMZ) and German Academic Exchange Service (DAAD), and their financial support we gratefully acknowledge.

REFERENCES

Amin, Md. N., Kaneco, S., Kitagawa, T., Begum, A., Katsumata, H., Suzuki, T. & Ohta, K. 2006 Removal of arsenic in aqueous solutions by adsorption onto waste rice husk. *Ind. Eng. Chem. Res.* **45**, 8105–8110.

Anirudhan, T. S., Nima, J., Sandeep, S. & Ratheesh, V. R. N. 2012 Development of an amino functionalized glycidylmethacrylate-grafted-titanium dioxide densified cellulose for the adsorptive removal of arsenic(V) from aqueous solutions. *Chem. Eng. J.* **209**, 362–371.

Aryal, M., Ziagova, M. & Kyriakides, M. L. 2010 Study on arsenic biosorption using Fe(III)-treated biomass of *Staphylococcus xylosus*. *Chem. Eng. J.* **162**, 178–185.

Baig, J. A., Kazi, T. G., Shah, A. Q., Kandhro, G. A., Afridi, H. I., Khan, S. & Kolachi, N. F. 2010 Biosorption studies on powder of stem of Acacia nilotica: removal of arsenic from surface water. *J. Hazard. Mater.* **178**, 941–948.

Barro-Traoré, F., Tiendrébéogo, S. R. M., Lallogo, S., Tiendrébéogo, S., Dabal, M. & Ouédraogo, H. 2008 Cutaneous manifestations of arsenicisme in Burkina-Faso: epidemiological and clinical features. *Mali Med.* **23**, 7–11.

Binod, P., Sindhu, R., Singhania, R. R., Vikram, S., Devi, L., Nagalakshmi, S., Kurien, N., Sukumaran, R. K. & Pandey, A. 2010 Bioethanol production from rice straw: an overview. *Bioresour. Technol.* **101**, 4767–4774.

Boonmee, A. 2012 Hydrolysis of various Thai agricultural biomasses using the crude enzyme from *Aspergillus Aculeatus* IIZUKA FR60 isolated from soil. *Braz. J. Microbiol.* **43**, 456–466.

Bordoloi, S., Nath, S. K., Gogoi, S. & Dutta, R. K. 2013 Arsenic and iron removal from groundwater by oxidation–coagulation at optimized pH: laboratory and field studies. *J. Hazard. Mater.* **260**, 618–626.

Bulut, G., Yenial, Ü., Emrecan, E. & Sirkeci, A. A. 2014 Arsenic removal from aqueous solution using pyrite. *J. Clean. Prod.* **84**, 626–632.

Chakravarty, S., Dureja, V., Bhattacharyya, G., Maity, S. & Bhattacharjee, S. 2002 Removal of arsenic from groundwater using low cost ferruginous manganese ore. *Water Res.* **36**, 625–632.

Choong, T. S. Y., Chuah, T. G., Robiah, Y., Gregory Koay, F. L. & Azni, I. 2007 Arsenic toxicity, health hazards and removal techniques from water: an overview. *Desalination* **217**, 139–166.

Correa, J. R., Bordallo, E., Canetti, D., León, V., Otero-Díaz, L. C., Negro, C., Gomez, A. & Saez-Puche, R. 2010 Structure and superparamagnetic behaviour of magnetite nanoparticles in cellulose beads. *Mater. Res. Bull.* **45**, 946–953.

Cui, H., Su, Y., Li, Q., Gao, S. & Shang, J. K. 2013 Exceptional arsenic (III,V) removal performance of highly porous, nanostructured ZrO_2 spheres for fixed bed reactors and the full-scale system modeling. *Water Res.* **47**, 6258–6268.

Dupont, L., Jolly, G. & Aplincourt, M. 2007 Arsenic adsorption on lignocellulosic substrate loaded with ferric ion. *Environ. Chem. Lett.* **5**, 125–129.

Dutta, P. K., Ray, A. K., Sharma, V. K. & Millero, F. J. 2004 Adsorption of arsenate and arsenite on titanium dioxide suspensions. *J. Colloid Interface Sci.* **278**, 270–275.

Elizalde-Gonzalez, M. P., Mattusch, J. & Wennrich, R. 2001 Application of natural zeolites for preconcentration of arsenic species in water samples. *J. Environ. Monit.* **3**, 22–26.

Elizalde-Gonzalez, M. P., Mattusch, J. & Wennrich, R. 2008 Chemically modified maize cobs waste with enhanced adsorption properties upon methyl orange and arsenic. *Bioresour. Technol.* **99**, 5134–5139.

Farook, A., Saraswathy, B. & Phee-Lee, W. 2006 Rice husk ash silica as a support material for ruthenium based heterogenous catalyst. *J. Phys. Sci.* **17**, 1–13.

Fernandez-Bolanos, J., Felizon, B., Heredia, A., Guillen, R. & Jimenez, A. 1999 Characterization of the lignin obtained by alkaline delignification and of the cellulose residue from steam-exploded olive stones. *Bioresour. Technol.* **68**, 121–132.

Gang, D. D., Deng, B. & Lin, L. 2010 As(III) removal using an iron-impregnated chitosan sorbent. *J. Hazard. Mater.* **182**, 156–161.

Guo, X. & Chen, F. 2005 Removal of arsenic by bead cellulose loaded with iron oxyhydroxide from groundwater. *Environ. Sci. Technol.* **39**, 6808–6818.

Gupta, A., Chauhan, V. S. & Sankararamakrishnan, N. 2009 Preparation and evaluation of iron–chitosan composites for removal of As(III) and As(V) from arsenic contaminated real life groundwater. *Water Res.* **43**, 3862–3870.

Han, C., Li, H., Pu, H., Yu, H., Deng, L., Huang, S. & Luo, Y. 2013 Synthesis and characterization of mesoporous alumina and their performances for removing arsenic(V). *Chem. Eng. J.* **217**, 1–9.

Hsu, T.-C., Guo, G.-L., Chen, W.-H. & Hwang, W.-S. 2010 Effect of dilute acid pretreatment of rice straw on structural properties and enzymatic hydrolysis. *Bioresour. Technol.* **101**, 4907–4913.

Jain, C. K. & Singh, R. D. 2012 Technological options for the removal of arsenic with special reference to South East Asia. *J. Environ. Manage.* **107**, 1–18.

Jeon, C.-S., Baek, K., Park, J.-K., Oh, Y.-K. & Lee, S.-D. 2009 Adsorption characteristics of As(V) on iron-coated zeolite. *J. Hazard. Mater.* **163**, 804–808.

Kalderis, D., Koutoulakis, D., Paraskeva, P., Diamadopoulos, E., Otal, E., Del Valle, J. O. & Fernandez-Pereira, C. 2008 Adsorption of polluting substances on activated carbons prepared from rice husk and sugarcane bagasse. *Chem. Eng. J.* **144**, 42–50.

Kanel, S. R., Choi, H., Kim, J.-Y., Vigneswaran, S. & Shim, W. G. 2006 Removal of arsenic (III) from groundwater using low-cost by-products-blast furnace slag. *Water Qual. Res. J. Can.* **41**, 130–139.

Karimi, K., Kheradmandinia, S. & Taherzadeh, M. J. 2006 Conversion of rice straw to sugars by dilute-acid hydrolysis. *Biomass Bioenerg.* **30**, 247–253.

Kim, S. & Dale, B. E. 2004 Global potential bioethanol production from wasted crops and crop residues. *Biomass Bioenerg.* **26**, 361–375.

Lenoble, V., Bouras, O., Deluchat, V., Serpaud, B. & Bollinger, J. C. 2002 Arsenic adsorption onto pillared clays and iron oxides. *J. Colloid Interface Sci.* **255**, 52–58.

Lenoble, V., Laclautre, C., Serpaud, B., Deluchat, V. & Bollinger, J.-C. 2004 As(V) retention and As(III) simultaneous oxidation and removal on a MnO_2-loaded polystyrene resin. *Sci. Total Environ.* **326**, 197–207.

Liu, C. F., Xu, F., Sun, J. X., Ren, L. J., Curling, S., Sun, R. C., Fowler, P. & Baird, M. S. 2006 Physicochemical characterization of cellulose from perennial ryegrass leaves (Lolium perenne). *Carbohydr. Res.* **341**, 2677–2687.

Lizama, K. A., Fletcher, T. D. & Sun, G. 2011 Removal processes for arsenic in constructed wetlands. *Chemosphere* **84**, 1032–1043.

Maji, S. K., Kao, Y.-H., Liao, P.-Y., Lin, Y.-J. & Liu, C.-W. 2013 Implementation of the adsorbent iron-oxide-coated natural rock (IOCNR) on synthetic As(III) and on real arsenic-bearing sample with filter. *Appl. Surf. Sci.* **284**, 40–48.

Mishra, A. K. & Ramaprabhu, S. 2011 Functionalized graphene sheets for arsenic removal and desalination of sea water. *Desalination* **282**, 39–45.

Mondal, P., Majumder, C. B. & Mohanty, B. 2006 Laboratory based approaches for arsenic remediation from contaminated water: recent developments. *J. Hazard. Mater. B* **137**, 464–479.

Munoz, J. A., Gonzalo, A. & Valiente, M. 2002 Arsenic adsorption by Fe(III)-loaded open-celled cellulose sponge. Thermodynamic and selectivity aspects. *Environ. Sci. Technol.* **36**, 3405–3411.

Namasivayam, C. & Sureshkumar, M. V. 2008 Removal of chromium (VI) from water and wastewater using surfactant modified coconut coir pith as a biosorbent. *Bioresour. Technol.* **99**, 2218–2225.

Nguyen, V. A., Bang, S., Viet, P. H. & Kim, K. W. 2009 Contamination of groundwater and risk assessment for arsenic exposure in Ha Nam province, Vietnam. *Environ. Int.* **35**, 466–472.

Pehlivan, E., Tran, T. H., Ouédraogo, W. K. I., Schmidt, C., Zachmann, D. & Bahadir, M. 2013 Removal of As(V) from aqueous solutions by iron coated rice husk. *Fuel Process. Technol.* **106**, 511–517.

Ranjan, D., Talat, M. & Hasan, S. H. 2009 Biosorption of arsenic from aqueous solution using agricultural residue 'rice polish'. *J. Hazard Mater.* **166**, 1050–1059.

Rau, I., Gonzalo, A. & Valiente, M. 2003 Arsenic(V) adsorption by immobilized iron mediation. Modeling of the adsorption process and influence of interfering anions. *React. Funct. Polym.* **54**, 85–94.

Sahiner, N., Ozay, O., Aktas, N., Blake, D. A. & John, V. T. 2011 Arsenic(V) removal with modifiable bulk and nano p(4-vinylpyridine)-based hydrogels: the effect of hydrogel sizes and quarternization agents. *Desalination* **279**, 344–352.

Sing, K. S. W., Everett, D. H., Haul, R. A. W., Moscou, L., Pierotti, R. A., Rouquerol, J. & Siemieniewska, T. 1985 Reporting physisorption data for gas/solid systems with special reference to the determination of surface area and porosity. *Pure Appl. Chem.* **57**, 603–619.

Singh, T. S. & Pant, K. K. 2004 Equilibrium, kinetics and thermodynamic studies for adsorption of As(III) on activated alumina. *Sep. Purif. Technol.* **36**, 139–147.

Smedley, P. L., Knudsen, J. & Maiga, D. 2007 Arsenic in groundwater from mineralised Proterozoic basement rocks of Burkina Faso. *Appl. Geochem.* **22**, 1074–1092.

Song, K., Kim, W., Suh, C.-Y., Shin, D., Ko, K.-S. & Ha, K. 2013 Magnetic iron oxide nanoparticles prepared by electrical wire explosion for arsenic removal. *Powder Technol.* **246**, 572–574.

Sun, J. X., Sun, X. F., Zhao, H. & Sun, R. C. 2004 Isolation and characterization of cellulose from sugarcane bagasse. *Polym. Degrad. Stab.* **84**, 331–339.

Thirunavukkarasu, O. S., Viraraghavan, T. & Subramanian, K. S. 2003 Arsenic removal from drinking water using iron oxide-coated sand. *Water Air Soil Pollut.* **142**, 95–111.

Urík, M., Littera, P., Ševc, J., Kolencík, M. & Cernanský, S. 2009 Removal of arsenic(V) from aqueous solutions using chemically modified sawdust of spruce (Picea abies): kinetics and isotherm studies. *Int. J. Environ. Sci. Tech.* **6**, 451–456.

Wan Ngah, W. S. & Hanafiah, M. A. K. M. 2008 Adsorption of copper on rubber (Hevea brasiliensis) leaf powder: kinetic, equilibrium and thermodynamic studies. *Biochem. Eng. J.* **39**, 521–530.

Wattanasiriwech, S., Wattanasiriwech, D. & Svasti, J. 2010 Production of amorphous silica nanoparticles from rice straw with microbial hydrolysis pretreatment. *J. Non-Cryst. Solids* **356**, 1228–1232.

Zhang, Y., Yang, M., Gao, Y., Wang, F. & Huang, X. 2003 Preparation and adsorption mechanism of rare earth-doped adsorbent for arsenic(V) removal from groundwater. *Science in China (Series B)* **46**, 252–258.

Zhang, W., Singh, P., Paling, E. & Delides, S. 2004 Arsenic removal from contaminated water by natural iron ores. *Miner. Eng.* **17**, 517–524.

Zhao, F. J., McGrath, S. P. & Meharg, A. A. 2010a Arsenic as a food chain contaminant: mechanisms of plant uptake and metabolism and mitigation strategies. *Annu. Rev. Plant Biol.* **61**, 535–559.

Zhao, R., Zhang, Z., Zhang, R., Li, M., Lei, Z., Utsumi, M. & Sugiura, N. 2010b Methane production from rice straw pretreated by a mixture of acetic–propionic acid. *Bioresour. Technol.* **101**, 990–994.

First received 6 October 2014; accepted in revised form 23 January 2015. Available online 13 March 2015